A Spectral-Domain Analysis of Periodically Nonuniform Coupled Microstrip Lines

FRANZ-JOSEF GLANDORF AND INGO WOLFF, FELLOW, IEEE

Abstract — **Periodically nonuniform coupled microstrip lines are analyzed on the basis of a numerical field calculation. As in the case of the single nonuniform microstrip line described in an earlier paper by the authors, Floquet's theorem is used to express all field quantities in terms of their spatial harmonics. The boundary value problem is formulated in a rigorous way and then solved using Galerkin's method in the Fourier-transform domain. Numerical and experimental results are presented.**

I. Introduction

In an earlier paper [1] the authors described a spectral-domain analysis of a single, periodically nonuniform microstrip line. In the introduction of that paper an overview was given which briefly described the literature in the area of nonuniform microstrip lines and how the method used by the authors deviated from earlier theories. Therefore this shall not be repeated here.

In this paper the problem of coupled, periodically nonuniform microstrip lines is investigated on the basis of the same spectral-domain calculation method as in [1]. These lines are interesting for the design of planar directional couplers with high directivity [2]–[4]. The fundamentals from the theory described in [1] will be used here without repetition, but new aspects which must be considered in the formulation of the tangential electric fields in the boundary between the substrate material and the air region as well as in the formulation of the surface current density in the metal strips will be studied in detail.

Numerical results will be presented for the case of two coupled microstrip lines with a sinusoidally varying coupling slot and for the case of a zigzag-shaped coupling slot. The convergence behavior will be discussed and numerical results will be compared to experiments.

II. Formulation of the Eigenvalue Problem

Coupled, periodically nonuniform microstrip lines with periodicity p as shown in Fig. 1 are investigated. It is assumed that the lines have the cross section shown in Fig. 1(a). All geometrical parameters and material parameters are defined in Fig. 1. The thickness of the top metallization (microstrip structure) is assumed to be zero. The two lines which form the coupled line structure are denoted as line 1 and line 2, respectively. The outer contours of the metallic strips are described by the periodic functions $w_o^{(1)}(z)$ and $w_o^{(2)}(z)$ and the inner contours by $w_i^{(1)}(z)$ and $w_i^{(2)}(z)$ (Fig. 1(b)). The widths of the two metal strips are $w^{(1)}(z) = |w_o^{(1)}(z) - w_i^{(1)}(z)|$ and $w^{(2)}(z) = |w_o^{(2)}(z) - w_i^{(2)}(z)|$. The functions $w_o^{(1),(2)}(z)$, $w_i^{(1),(2)}(z)$, and $w^{(1),(2)}(z)$ are periodic functions with periodicity p in relation to the z coordinate. As in the case of the single line, only structures with even contour functions will be investigated here (see arguments in [1]):

$$w_o^{(l)}(z) = w_o^{(l)}(-z),\ w_i^{(l)} = w_i^{(l)}(-z), \qquad l = 1,2. \quad (1)$$

Additionally only lines which fulfill the following conditions:

$$w_i^{(2)}(z) = -w_i^{(1)}(z + p/2),\ w_o^{(2)}(z) = -w_o^{(1)}(z + p/2) \quad (2)$$

shall be considered. These additional requirements, which are fulfilled by the coupled microstrip line shown in Fig. 1, drastically reduce the numerical expense in the computation process.

Line structures of the type shown in Fig. 1 are no longer symmetric with respect to the z axis as in the case of the single lines treated in [1]. Therefore the potential functions cannot be written as even or odd functions with respect to the x coordinate, as in the case of the single line [1, eq. (5)], and additional sine and cosine functions must be considered:

$$\phi_k^i(x,y) = \sum_{n=1}^{\infty} a_{nk}^i \cdot \sin\left(k_{ynk}^i (y + y^i)\right) \cdot \sin(k_{xn} x) + \sum_{m=0}^{\infty} c_{mk}^i \cdot \sin\left(k_{ymk}^i (y + y^i)\right) \cdot \cos(k_{xm} x)$$

$$\psi_k^i(x,y) = \sum_{n=1}^{\infty} b_{nk}^i \cdot \cos\left(k_{ynk}^i (y + y^i)\right) \cdot \cos(k_{xn} x) + \sum_{m=1}^{\infty} d_{mk}^i \cdot \cos\left(k_{ymk}^i (y + y^i)\right) \cdot \sin(k_{xm} x) \quad (3)$$

with $i = \mathrm{I}, \mathrm{II}$, $y^{\mathrm{I}} = d$, $y^{\mathrm{II}} = -h$, $k_{xn} = (n - 0.5)\pi/a$, $k_{xm} = m\pi/a$, and

$$k_{ynk}^{i2} = k_i^2 - k_{xn}^2 - \beta_k^2,$$

$$k_{ymk}^{i2} = k_i^2 - k_{xm}^2 - \beta_k^2, \quad k_i^2 = k_0^2 \epsilon_r^i.$$

Manuscript received February 9, 1987; revised July 29, 1987.

F. J. Glandorf was with the Department of Electrical Engineering, Universität Duisburg, West Germany. He now is with ANT Nachrichtentechnik, D-7150 Backnang, West Germany.

I. Wolff is with the Department of Electrical Engineering and Sonderforschungsbereich 254, Universität Duisburg, D-4100 Duisburg, West Germany.

IEEE Log Number 8718367.

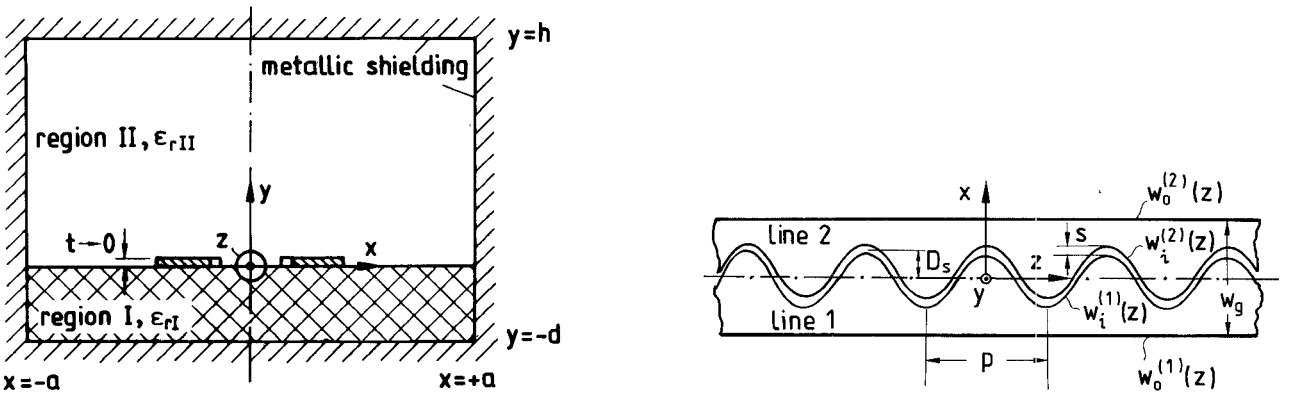

(a) (b)

Fig. 1. Nonuniform, coupled microstrip lines. (a) Cross-sectional view. (b) Example of two coupled lines with sinusoidal coupling slot structure.

The calculation of the electric and the magnetic field strength from the potential functions can be performed in the same way as in the case of the single line. Also, the components of the surface current density are no longer even or odd functions of the x coordinate, and the two-dimensional Fourier series for J_x and the J_z now must be written as

$$J_x = \sum_{k=-\infty}^{+\infty} \left\{ \sum_{n=1}^{\infty} J_{xnk} \sin(k_{xn}x) + \sum_{m=0}^{\infty} J_{xmk} \cos(k_{xm}x) \right\} e^{j\beta_k z}$$

$$J_z = \sum_{k=-\infty}^{+\infty} \left\{ \sum_{n=1}^{\infty} J_{znk} \cos(k_{xn}x) + \sum_{m=1}^{\infty} J_{zmk} \sin(k_{xm}x) \right\} e^{j\beta_k z}. \quad (4)$$

The x and z components of the electric field strength in the substrate surface, considering the total potential functions in (3), are

$$E_x|_{y=0} = \sum_{k=-\infty}^{+\infty} \left\{ \sum_{n=1}^{\infty} (j\Gamma_{xxnk} J_{xnk} + \Gamma_{xznk} J_{znk}) \sin(k_{xn}x) + \sum_{m=0}^{\infty} (j\Gamma_{xxmk} J_{xmk} + \Gamma_{xzmk} J_{zmk}) \cdot \cos(k_{xm}x) \right\} e^{j\beta_k z}$$

$$E_z|_{y=0} = \sum_{k=-\infty}^{+\infty} \left\{ \sum_{n=1}^{\infty} (-\Gamma_{xznk} J_{xnk} + j\Gamma_{zznk} J_{znk}) \cdot \cos(k_{xn}x) + \sum_{m=1}^{\infty} (-\Gamma_{xzmk} J_{xmk} + j\Gamma_{zzmk} J_{zmk}) \cdot \sin(k_{xm}x) \right\} e^{j\beta_k z}. \quad (5)$$

The coefficients Γ_{xxnk}, Γ_{xznk}, and Γ_{zznk} are identical with those given in [1, eq. (8b)]. The coefficients Γ_{xxmk}, Γ_{xzmk}, and Γ_{zzmk} can also be calculated from [1, eq. (8b)] if the index n is replaced by m, and additionally the coefficients Γ_{xzmk} are multiplied by -1.

As in the case of the single line, the surface current density is developed into a series using a functional system which will be described later [1, eq. (9)]. If J_u is the component of the surface current density normal to the strip contour and J_v is the component parallel to it,

$$\begin{bmatrix} J_u \\ J_v \end{bmatrix} = \begin{bmatrix} \cos(\alpha(x,z)) & -\sin(\alpha(x,z)) \\ \sin(\alpha(x,z)) & \cos(\alpha(x,z)) \end{bmatrix} \begin{bmatrix} J_x \\ J_z \end{bmatrix} = \overleftrightarrow{T} \begin{bmatrix} J_x \\ J_z \end{bmatrix} \quad (6)$$

with $\alpha(x,z)$ given by [1, eq. (15)]. J_u must vanish on the strip contour. J_v must fulfill the edge condition [6], i.e., for the infinitely thin metallization it must have a singularity of the order $O(\rho^{-0.5})$ at the strip edge. The edge condition is not essentially changed in the case of curved edges [7]. A series description of these two components now is

$$J_u = \sum_{\nu=1}^{2} \sum_{i=1}^{\infty} \sum_{l=-\infty}^{+\infty} u_{il}^{(\nu)} X_i^{(\nu)}(x,z) e^{j\beta_l z}$$

$$J_v = \sum_{\nu=1}^{2} \sum_{i=1}^{\infty} \sum_{l=-\infty}^{+\infty} v_{il}^{(\nu)} Z_i^{(\nu)}(x,z) e^{j\beta_l z} \quad (7)$$

where the index ν describes lines 1 and 2, respectively. Because of the varying line width, the expansion functions $X_i^{(\nu)}(x,z)$ and $Z_i^{(\nu)}(x,z)$ must depend on the z coordinate. The expansion functions $X_i^{(1)}(x,z)$ and $Z_i^{(1)}(x,z)$ have nonzero values only on line 1 and vanish otherwise, whereas the functions $X_i^{(2)}(x,z)$ and $Z_i^{(2)}(x,z)$ have nonzero values only on line 2. If all the conditions which have been formulated for the eigenvalue problem above are taken into account, the coefficients of the two-dimensional

Fouriers series expansion (4) are found from

$$J_{xnk} = \sum_{\nu=1}^{2} \sum_{\iota=1}^{\infty} \sum_{l=-\infty}^{+\infty} u_{il}^{(\nu)} CXS_{\iota nlk}^{(\nu)} + jv_{il}^{(\nu)} SZS_{\iota nlk}^{(\nu)}$$

$$J_{znk} = \sum_{\nu=1}^{2} \sum_{\iota=1}^{\infty} \sum_{l=-\infty}^{+\infty} -ju_{il}^{(\nu)} SXC_{\iota nlk}^{(\nu)} + v_{il}^{(\nu)} CZC_{\iota nlk}^{(\nu)}$$

$$J_{xmk} = \sum_{\nu=1}^{2} \sum_{\iota=1}^{\infty} \sum_{l=-\infty}^{+\infty} u_{il}^{(\nu)} CXC_{\iota mlk}^{(\nu)} + jv_{il}^{(\nu)} SZC_{\iota mlk}^{(\nu)}$$

$$J_{zmk} = \sum_{\nu=1}^{2} \sum_{\iota=1}^{\infty} \sum_{l=-\infty}^{+\infty} -ju_{il}^{(\nu)} SXS_{\iota mlk}^{(\nu)} + v_{il}^{(\nu)} CZS_{\iota mlk}^{(\nu)} \quad (8)$$

with the abbreviations given in the Appendix. Due to the restrictive conditions (1) and (2) which have been assumed for the line geometry, special relations between the abbreviations are valid (see Appendix, eq. (A2)).

The two metal strips on top of the substrate and the ground metallization form a three-conductor system. Therefore two possible fundamental modes must exist on this line structure. If the amplitude D_s of the slot contour function (Fig. 1) decreases to zero, these solutions must converge to the fundamental even and odd mode of two uniform coupled microstrip lines. Therefore these modes shall be called even and odd also in the case of the nonuniform coupled lines, despite the fact that the electromagnetic field does not have an even or odd symmetry with respect to the z axis.

For the fundamental even mode the condition

$$u_{il}^{(2)} = -(-1)^l u_{il}^{(1)} \qquad v_{il}^{(2)} = (-1)^l v_{il}^{(1)} \quad (9)$$

and for the fundamental odd mode the condition

$$u_{il}^{(2)} = (-1)^l u_{il}^{(1)} \qquad v_{il}^{(2)} = -(-1)^l v_{il}^{(1)} \quad (10)$$

must be valid because of symmetry aspects. Using these relations, the Fourier series coefficients given in (8) again can be simplified.

Using the Fourier series coefficients of the surface current density given in (8), the x and z components of the electric field in the surface of the substrate material can be found as

$$E_x|_{y=0} = \sum_{\iota=1}^{\infty} \sum_{l=-\infty}^{+\infty} \sum_{k=-\infty}^{+\infty} 2\Bigg[\delta_k \sum_{n=1}^{\infty} \left(ju_{il}^{(1)} P_{\iota nlk} + v_{il}^{(1)} R_{\iota nlk}\right) \sin(k_{xn}x) + \bar{\delta}_k \sum_{m=0}^{\infty} \left(ju_{il}^{(1)} P_{\iota mlk} + v_{il}^{(1)} R_{\iota mlk}\right) \cos(k_{xm}x)\Bigg] e^{j\beta_k z}$$

$$E_z|_{y=0} = \sum_{\iota=1}^{\infty} \sum_{l=-\infty}^{+\infty} \sum_{k=-\infty}^{+\infty} 2\Bigg[\delta_k \sum_{n=1}^{\infty} \left(u_{il}^{(1)} Q_{\iota nlk} + jv_{il}^{(1)} S_{\iota nlk}\right) \cos(k_{xn}x) + \bar{\delta}_k \sum_{m=1}^{\infty} \left(u_{il}^{(1)} Q_{\iota mlk} + jv_{il}^{(1)} S_{\iota mlk}\right) \sin(k_{xm}x)\Bigg] e^{j\beta_k z} \quad (11)$$

with

$\delta_k = 1$ for k even and even modes or k odd and odd modes

$\delta_k = 0$ for k even and odd modes or k odd and even modes

and

$\bar{\delta}_k = 1$ for k even and odd modes or k odd and even modes

$\bar{\delta}_k = 0$ for k odd and odd modes or k even and even modes.

The abbreviations again are given in the Appendix (eq. (A3)).

The total electromagnetic field of coupled nonuniform microstrip lines is not symmetrical with respect to the x coordinate, as it is in the case of uniform symmetric coupled microstrip lines. Nevertheless each space harmonic partial field (see [1]) contributes only an even or an odd part to the total field, as can be seen from (11). Therefore the even and the odd mode on lines which fulfill the conditions given in (1) and (2) can be computed separately.

The further solution of the eigenvalue problem is nearly identical to the case of the single line [1]. Galerkin's method is used for the even modes and the odd modes separately. The expansion functions which are applied to (5) are

$$X_i^{(1)} = \sin(i\pi\xi) \cdot s_m(\xi)$$

$$Z_i^{(1)} = \cos((i-1)\pi\xi) \cdot s_m(\xi) \quad (12)$$

with Maxwell's edge function s_m

$$s_m(\xi) = \frac{1}{\sqrt{1-4(\xi-0.5)^2}} \quad \text{and} \quad \xi = \left(x - w_o^{(1)}(z)\right)/w^{(1)}(z) \quad (13)$$

for $w_o^{(1)}(z) \leqslant x \leqslant w_i^{(1)}(z)$.

The functions given in (12) are developed into Fourier series. The integration with respect to the x direction can be performed analytically; with respect to the z axis it must be done numerically.

From the application of Galerkin's method, an infinite equation system with a real and symmetric coefficient matrix is derived for the even and odd modes. The series expansions used in this equation system will be truncated at indices I, L, and N, as in the case of the single line [1]. Again, the series for index k are truncated at $-(K+L)$ and $+(K+L)$. Elements which contain Fourier coefficients of expansion functions with an index having an absolute value larger than K are set to zero. The additional series for index m will be truncated at the same index N as the series for index n. Two truncation indices I_u and I_v are used for the series of the J_u and the J_v components, where I_v should be larger than I_u. As will be explained later, the choice of $I_u = 3$ and $I_v = 6$ is sufficient for convergence. Therefore the convergence behavior of the method only needs to be discussed in relation to the truncation indices N, K of the Fourier series of the expansion functions and the truncation index L of the Fourier series describing the surface current density.

The solutions of the eigenvalue problem again are determined by searching the zeros of the determinant of the

finite system matrix. As in the case of the single lines, in addition to microstrip modes, waveguide modes can be found as solutions of the closed boundary value problem shown in Fig. 1. All solutions have adjoint higher order solutions with a phase coefficient which is changed by $2\mu\pi/p$ ($\mu = \pm 1, 2, \cdots$). The solutions can be classified using the same method as in the case of the single line.

III. The Convergence of the Method

The convergence of the method described is analyzed using a coupled line structure with a sinusoidal contour function of the coupling slot, as shown in Fig. 1(b). The geometrical parameters of the line structure used here are $w_g = |w_o^{(1)} - w_o^{(2)}| = 10.0$ mm, $s = 0.42$ mm, $p = 8.75$ mm, and $D_s = 1.0$ mm. The substrate material has a height $h = 1.56$ mm and a relative dielectric constant $\epsilon_r = 2.32$.

As in the case of the nonuniform single microstrip line, the accuracy of the computed effective dielectric constant depends on the number of expansion functions as well as the number of Fourier coefficients which have been taken into account for calculating the surface current density. Additionally, it depends on the accurate description of the expansion functions in the spectral domain, i.e., on the number of coefficients considered of the Fourier series for the electromagnetic fields.

Concerning the transformation of the expansion functions into the spectral domain, it must be considered that not only the transformation of the expansion functions itself but also the transformation of the contour function of the coupling slot must be carried out with sufficient accuracy. For the transformation of the expansion functions into the spectral domain, in the x direction $N = \max(4 * I_v * F * a/w_{\min}, 4a/s)$ spectral terms will be considered. Here $w_{\min}$ is the smallest strip width of lines 1 and 2, and $2a$ is the width of the metallic shielding. F is a numerical factor describing the value of N. It is found that for the expansion functions given in (12) the convergence of the method is achieved for $F = 2$. If it is required that the error of the effective dielectric constant be less than 0.2 percent, six v components ($I_v = 6$) and three u components ($I_u = 3$) (see (7)) of the surface current density must be taken into account.

Fig. 2 shows the error of the numerically determined effective dielectric constant in relation to the cutoff index K of the Fourier series expansion of the electromagnetic field a) for the phase coefficient $\beta_N = \beta p/\pi = 0.1$ and b) for $\beta_N = 0.25$. The error is calculated by comparing the actual value of the effective dielectric constant with its value for $K = 20$ and $L = 7$. Again, as in the case of the single nonuniform line [1], the frequency dependence of the convergence can be recognized. For values of the normalized phase coefficient $\beta_N = 0.25$ ($\lambda = 8p$, $f \approx 3$ GHz), the convergence of the fundamental odd mode in particular is much better than in the case of $\beta_N = 0.1$. As a result it is found that for a sure convergence, $K = 1.5 * N * D_s/a$ Fourier coefficients have to be considered in the transformation of the expansion functions into the spectral domain. For the line structure considered this means that the results are of satisfactory accuracy if $K = 15$.

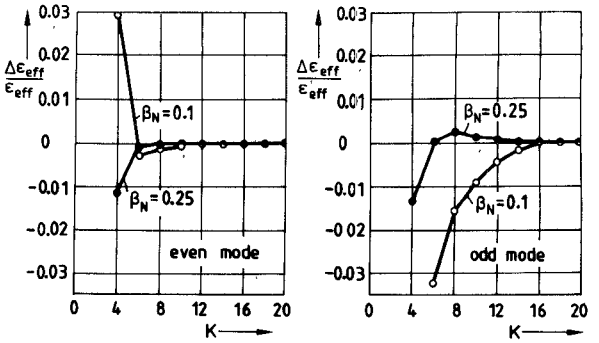

Fig. 2. The convergence of the numerically determined effective dielectric constants of two coupled microstrip lines with a sinusoidal coupling slot structure as a function of the truncation index K of the Fourier series describing the electromagnetic fields. Line parameters: $w_g = |w_o^{(1)} - w_o^{(2)}| = 10.0$ mm, $s = 0.42$ mm, $p = 8.75$ mm, $D_s = 1.0$ mm. Substrate material: $d = 1.56$ mm, $\epsilon_r = 2.32$.

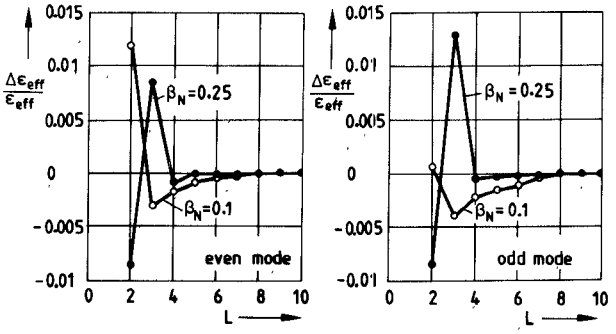

Fig. 3. The convergence of the numerically determined effective dielectric constants of two coupled microstrip lines with a sinusoidal coupling slot structure as a function of the truncation index L of the Fourier series describing the surface current density. For line and substrate parameters, see Fig. 2.

Fig. 3 shows the relative error of the numerically determined effective dielectric constant of the fundamental even and odd modes in relation to the number L of the Fourier coefficients of the surface current density considered. The actual values are compared to those values which have been computed with $K = 20$ and $L = 10$. The frequency dependence of the convergence is not as clear in this case as in Fig. 2. The relative error of the numerically determined effective dielectric constant is less than 0.05 percent if $L \geqslant 7$.

Figs. 4 and 5 show equivalent results for the convergence in the case of a coupled microstrip line with a zigzag-shaped coupling slot. All geometrical parameters of this line are identical with those of the line with sinusoidally shaped coupling slot. As can be seen from Fig. 4, the cutoff index K must be larger than in the case of the sinusoidally shaped coupling slot to reach the same relative error for the numerically determined effective dielectric constant. In this case the cutoff index K must be $K = 2 * N * D_s/a$, and the result is reached for $K \geqslant 20$. A similar result is found from Fig. 5, where the dependence of the convergence on the number L of Fourier coefficients for the surface current description is shown. In this case the error of the numerically determined effective dielectric constant is less than 0.2 percent for $L \geqslant 8$. For values of $L \leqslant 7$ the relative error is much larger than in the

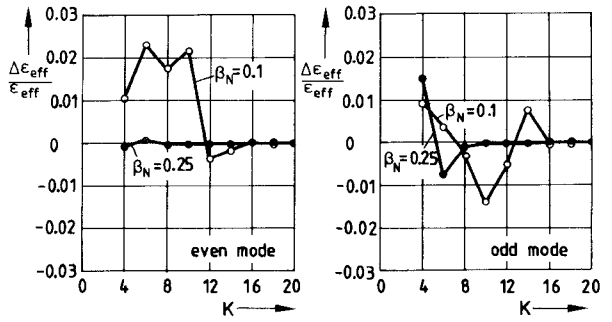

Fig. 4. The convergence of the numerically determined effective dielectric constants of two coupled microstrip lines with a zigzag coupling slot structure as a function of the truncation index K of the Fourier series describing the electromagnetic fields. Line and substrate parameters are given in Fig. 2.

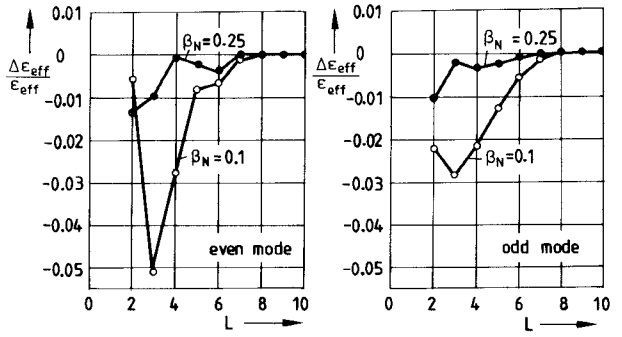

Fig. 5. The convergence of the numerically determined effective dielectric constants of two coupled microstrip lines with a zigzag coupling slot structure as a function of the truncation index L of the Fourier series describing the surface current density. Line and substrate parameters are given in Fig. 2.

case of the line with sinusoidally shaped coupling slot. The relative errors given in Figs. 4 and 5 are estimated by comparing the actual values of ϵ_{eff} with those computed for $K = 20$ and $L = 10$.

IV. Numerical and Experimental Results

In the case of the coupled nonuniform microstrip lines, primary interest in the investigation is not in the frequency dependence of the line parameters itself but (e.g. for the design of directional couplers) in the fact that the phase velocities of the fundamental even and odd modes may be equalized by a proper choice of the coupling slot contour. This effect has been used for the realization of phase shifters [3] and directional couplers [2]–[4] in microstrip.

In Fig. 6 the effective dielectric constant of three different coupled microstrip lines on polyguide substrate material ($\epsilon_r = 2.32$, $h = 1.56$ mm) and with a sinusoidal contour of the coupling slot is shown in relation to the amplitude D_s of the contour. The geometrical parameters of the lines are identical with those of the lines discussed in Section III ($s = 0.42$ mm, $w_g = 10.0$ mm). Lines with periodicities of $p = 8.75$ mm, $p = 11.67$ mm, and $p = 17.5$ mm are investigated at a wavelength of $\lambda = 70$ mm, which means that the adjoint normalized phase coefficients are $\beta_N = \beta p/\pi = 0.25$, 0.33, and 0.5, respectively.

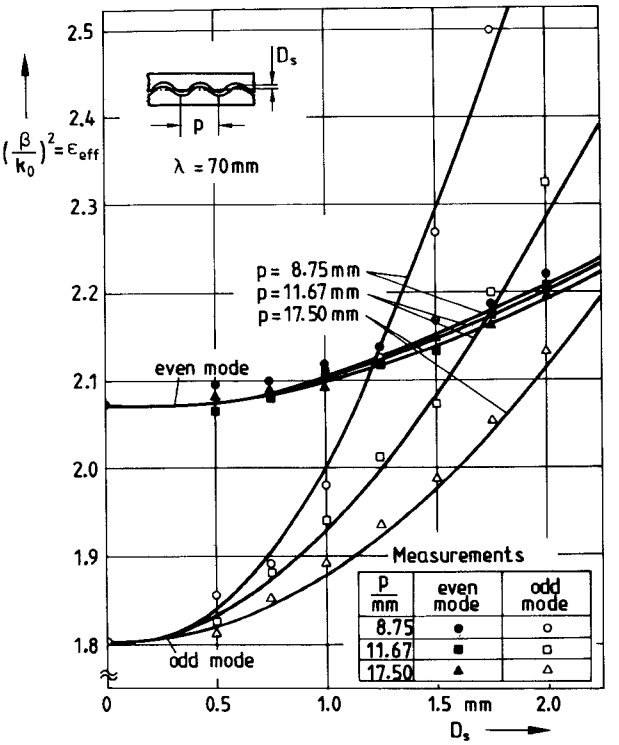

Fig. 6. Theoretical and experimental results for the effective dielectric constants of the even and the odd mode on two coupled, nonuniform microstrip lines with a sinusoidal coupling slot structure as a function of the "amplitude" D_s (see Fig. 1) and with the periodicity p as a parameter.

As can be seen from Fig. 6, the effective dielectric constant of the fundamental even mode is not greatly influenced by the amplitude D_s, whereas that of the fundamental odd mode is strongly dependent on D_s. For the example considered the effective dielectric constant of the fundamental even mode is changed by only 7 percent if D_s increases from 0 to 2 mm; additionally the periodicity does not have a big influence on ϵ_{eff} of the even mode. This effect can be explained by the fact that the electromagnetic field of the odd mode is much more concentrated near the coupling slot than that of the even mode. Therefore the influence of the slot contour on the phase velocity of the odd mode is large, while the influence on the even mode parameters is only small. Physically this means that for the odd mode a big part of the electromagnetic energy is traveling along the slot structure whereas the even mode to a first approximation travels along the z axis, as in the case of uniform coupled lines. This also means that the odd mode exhibits more distinctively the typical slow wave properties, e.g. the effective dielectric constant of the odd mode becomes larger than $\epsilon_r = 2.32$ for $D_s \approx 1.5$ mm, whereas the increase of ϵ_{eff} of the even mode is much smaller (Fig. 6, cf. also [1]).

In Fig. 7 similar results are shown for the example of a coupled microstrip line with a zigzag-shaped coupling slot. The geometrical parameters are the same as in the case of the line with a sinusoidal slot contour function. Initially the results shown in Figs. 6 and 7 seem identical, but a comparison in detail shows that the influence of the slot

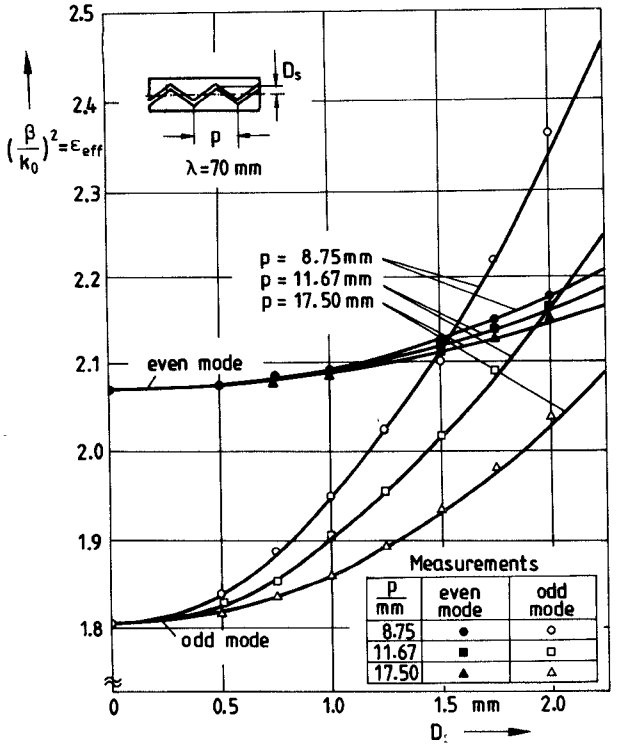

Fig. 7. Theoretical and experimental results for the effective dielectric constants of the even and the odd mode on two coupled, nonuniform microstrip lines with a zigzag coupling slot structure as a function of the "amplitude" D_s (see Fig. 1) and with the periodicity p as a parameter.

amplitude D_s on the effective dielectric constant of the odd mode is larger for Fig. 6. The physical interpretation of this effect is that the odd mode fields (to a first approximation) travel along the coupling slot contour, and therefore the effective distance which they have to cover is larger in the case of the sinusoidal contour than the zigzag-shaped contour.

Some experimental results from measurements are also given in Figs. 6 and 7. The resonator method proposed by Wolff [5] was used for measuring the effective dielectric constants of the even and the odd modes. This method eliminates the influence of the end effects of the resonator structure by comparing the measured results of two resonators of different lengths. The resonators must have identical geometries and the ratios of their lengths must be the ratio of two integer numbers. This means in the case of periodically nonuniform microstrip lines that only resonators of lengths $l_1 = np$ and $l_2 = mp$ with $n, m = 1, 2, 3, \cdots$ and $n \neq m$ can be used. Therefore only measurement results at certain wavelengths or frequencies which are determined by the periodicity p of the line can be obtained. The measurement results in Figs. 6 and 7 have been obtained by using resonators with lengths of 70 mm and 35 mm. The long resonators were used as one-wavelength resonators whereas the shorter ones were used as half-wavelength resonators.

As can be seen from Fig. 6 and Fig. 7, the agreement between theory and measurements is good. The agreement is better in the case of the zigzag-shaped coupling slot contour because at the time of measurements no computer-controlled mask cutter was available and the sinusoidal contour function could be realized only with low accuracy.

V. Conclusions

Periodically nonuniform microstrip lines have been analyzed on the basis of a numerical field calculation. Floquet's theorem is used to express all field quantities in terms of their spatial harmonics. The boundary value problem has been formulated in a rigorous way and has then been solved using Galerkin's method in the Fourier-transform domain. The convergence of the method and numerical results have been discussed. These have been compared to experiments for the effective dielectric constants of the even and the odd modes. As a result it has been shown that the even- and odd-mode effective dielectric constants may be equalized for certain line geometries. The numerical expense of the applied method is high. Therefore the method in its present form will not be usable in CAD programs for microwave circuits.

Appendix

The abbreviations used in (8) are

$$CXS_{inlk}^{(\nu)} = \frac{(-1)^{\nu+1}}{ap} \int_{z_0}^{z_0+p} \int_{w_o^{(\nu)}(z)}^{w_i^{(\nu)}(z)} \cos(\alpha^{(\nu)}) X_i^{(\nu)} \cdot \sin(k_{xn}x) e^{j2\pi(l-k)z/p}\, dx\, dz$$

$$SZS_{inlk}^{(\nu)} = \frac{(-1)^{\nu+1}}{ap} \int_{z_0}^{z_0+p} \int_{w_o^{(\nu)}(z)}^{w_i^{(\nu)}(z)} -j \sin(\alpha^{(\nu)}) Z_i^{(\nu)} \cdot \sin(k_{xn}x) e^{j2\pi(l-k)z/p}\, dx\, dz$$

$$SXC_{inlk}^{(\nu)} = \frac{(-1)^{\nu+1}}{ap} \int_{z_0}^{z_0+p} \int_{w_o^{(\nu)}(z)}^{w_i^{(\nu)}(z)} -j \sin(\alpha^{(\nu)}) X_i^{(\nu)} \cdot \cos(k_{xn}x) e^{j2\pi(l-k)z/p}\, dx\, dz$$

$$CZC_{inlk}^{(\nu)} = \frac{(-1)^{\nu+1}}{ap} \int_{z_0}^{z_0+p} \int_{w_o^{(\nu)}(z)}^{w_i^{(\nu)}(z)} \cos(\alpha^{(\nu)}) Z_i^{(\nu)} \cdot \cos(k_{xn}x) e^{j2\pi(l-k)z/p}\, dx\, dz$$

$$CXC_{imlk}^{(\nu)} = \frac{(-1)^{\nu+1}}{ap} \int_{z_0}^{z_0+p} \int_{w_o^{(\nu)}(z)}^{w_i^{(\nu)}(z)} \cos(\alpha^{(\nu)}) X_i^{(\nu)} \cdot \cos(k_{xm}x) e^{j2\pi(l-k)z/p}\, dx\, dz$$

$$SZC_{imlk}^{(\nu)} = \frac{(-1)^{\nu+1}}{ap} \int_{z_0}^{z_0+p} \int_{w_o^{(\nu)}(z)}^{w_i^{(\nu)}(z)} -j \sin(\alpha^{(\nu)}) Z_i^{(\nu)} \cdot \cos(k_{xm}x) e^{j2\pi(l-k)z/p}\, dx\, dz$$

$$SXS_{imlk}^{(\nu)} = \frac{(-1)^{\nu+1}}{ap} \int_{z_0}^{z_0+p} \int_{w_o^{(\nu)}(z)}^{w_i^{(\nu)}(z)} -j \sin(\alpha^{(\nu)}) X_i^{(\nu)} \cdot \sin(k_{xm}x) e^{j2\pi(l-k)z/p}\, dx\, dz$$

$$CZS_{imlk}^{(\nu)} = \frac{(-1)^{\nu+1}}{ap} \int_{z_0}^{z_0+p} \int_{w_o^{(\nu)}(z)}^{w_i^{(\nu)}(z)} \cos(\alpha^{(\nu)}) Z_i^{(\nu)} \cdot \sin(k_{xm}x) e^{j2\pi(l-k)z/p}\, dx\, dz. \quad \text{(A1)}$$

The coefficients are connected by

$$
\begin{aligned}
CXS^{(2)}_{inlk} &= -(-1)^{(l-k)} CXS^{(1)}_{inlk} \\
CXC^{(2)}_{imlk} &= (-1)^{(l-k)} CXC^{(1)}_{imlk} \\
CZC^{(2)}_{inlk} &= (-1)^{(l-k)} CZC^{(1)}_{inlk} \\
CZS^{(2)}_{imlk} &= -(-1)^{(l-k)} CZS^{(1)}_{imlk} \\
SXC^{(2)}_{inlk} &= -(-1)^{(l-k)} SXC^{(1)}_{inlk} \\
SXS^{(2)}_{imlk} &= (-1)^{(l-k)} SXS^{(1)}_{imlk} \\
SZS^{(2)}_{inlk} &= (-1)^{(l-k)} SZS^{(1)}_{inlk} \\
SZC^{(2)}_{imlk} &= -(-1)^{(l-k)} SZC^{(1)}_{imlk}. \qquad \text{(A2)}
\end{aligned}
$$

The abbreviations used in (11) are

$$
\begin{aligned}
P_{inlk} &= \Gamma_{xxnk} CXS^{(1)}_{inlk} - \Gamma_{xznk} SXC^{(1)}_{inlk} \\
Q_{inlk} &= \Gamma_{zznk} SXC^{(1)}_{inlk} - \Gamma_{xznk} CXS^{(1)}_{inlk} \\
R_{inlk} &= \Gamma_{xznk} CZC^{(1)}_{inlk} - \Gamma_{xxnk} SZS^{(1)}_{inlk} \\
S_{inlk} &= \Gamma_{zznk} CZC^{(1)}_{inlk} - \Gamma_{xznk} SZS^{(1)}_{inlk} \\
P_{imlk} &= \Gamma_{xxmk} CXC^{(1)}_{imlk} - \Gamma_{xzmk} SXS^{(1)}_{imlk} \\
Q_{imlk} &= \Gamma_{zzmk} SXS^{(1)}_{imlk} - \Gamma_{xzmk} CXC^{(1)}_{imlk} \\
R_{imlk} &= \Gamma_{xzmk} CZS^{(1)}_{imlk} - \Gamma_{xxmk} SZC^{(1)}_{imlk} \\
S_{imlk} &= \Gamma_{zzmk} CZS^{(1)}_{imlk} - \Gamma_{xzmk} SZC^{(1)}_{imlk}. \qquad \text{(A3)}
\end{aligned}
$$

REFERENCES

[1] F.-J. Glandorf and I. Wolff, "A spectral domain analysis of periodically nonuniform microstrip lines," *IEEE Trans. Microwave Theory Tech.*, vol. MTT-33, pp. 336–343, Mar. 1987.

[2] A. Podell, "A high directivity microstrip coupler technique," in *1970 IEEE GMTT Int. Microwave Symp. Dig.* (Newport Beach, CA), May 1970, pp. 33–36.

[3] J. L. Taylor and D. D. Prigel, "Wiggley phase shifters and directional couplers for radio-frequency hybrid-microcircuit applications," *IEEE Trans. Parts, Hybrids and Packaging*, vol. PHP-12, pp. 317–323, 1976.

[4] F. C. de Ronde, "Wide-band high directivity in MIC proximity couplers by planar means," in *1980 IEEE MTT-S Int. Microwave Symp. Dig.* (Washington, DC), May 1980, pp. 480–481.

[5] I. Wolff, "Messung der effektiven Dielektrizitätszahlen des geraden und des ungeraden Wellentyps auf gekoppelten Microstrip-Leitungen," *Nachrichtentech. Z.*, vol. 27, pp. 30–34, 1974.

[6] B.-H. Liu, "On the behaviour of electromagnetic fields at twisted edges and on conical vertexes in inhomogeneous medium, *Arch. Elektrotech.*, vol. 60, pp. 249–258, 1978.

Franz J. Glandorf was born in Ostercappeln, West Germany, in 1949. He received the Dipl.-Ing. degree in electrical engineering from the Technical University Aachen in 1975, and the Dr.-Ing. degree from Duisburg University, West Germany, in 1982.

From 1975 to 1982, he was with the Department of Electrical Engineering at Duisburg University. His main research activities were numerical investigations of planar microwave structures. Since 1982, he has been with ANT Nachrichtentechnik, Backnang, West Germany. He is currently working on passive microwave components, mixers, and oscillators for space applications.

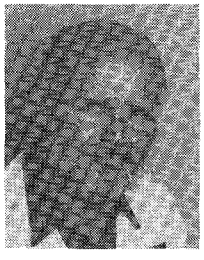

Ingo Wolff (M'75–SM'85–F'88) was born in Köslin, Germany, in 1938. He received the Dipl.-Ing. degree, the Dr.-Ing. degree, and the Habilitation degree from the Technical University Aachen, West Germany, in 1964, 1967, and 1970, respectively.

He was an Associate Professor for High-Frequency Techniques at the Technical University Aachen from 1970 to 1974. Since 1974, he has been a Full Professor for Electromagnetic Field Theory at Duisburg University, Duisburg, West Germany. He has carried out research work on millimeter-wave techniques, ferrite components, computer-aided design of planar microwave components, microwave integrated circuits, and planar microwave antennas.